Immunogenetics: Open Access

OPEN ACCESS Freely available online

Research Article

Constructing the Immune Related Prognosis Score to Predict the Benefit of Immunotherapy in Colorectal Cancer

Jun Xiang[1], JunHu Li[2], XiaoNan Cheng[3], HanQing Hu[1], Lei Yu[1*], GuiYu Wang[1*]

[1]Department of Colorectal Surgery, The Second Affiliated Hospital of Harbin Medical University, Harbin, China;[2]Department of Anorectal Surgery, The Second Affiliated Hospital of Harbin Medical University, Harbin, China;[3]Department of Immunogenetics, The Second Affiliated Hospital of Harbin Medical University, Harbin, China

ABSTRACT

Background: Since Food and Drug Administration (FDA) approved immune checkpoint inhibitors for the treatment of colorectal cancer in 2017, there have been significant differences in the response of colorectal cancer patients to immune checkpoint inhibitors. In order to achieve better clinical benefits of colorectal cancer patients in immunotherapy, we urgently need to find a biomarker to evaluate whether colorectal cancer patients respond to immunotherapy. In this research, we aimed to explore a biomarker to predict the efficacy of immunotherapy for colorectal cancer patients.

Materials and methods: We collected the expression profiles and clinical information of more than 1800 colorectal cancer patients in 6 cohorts in Gene Expression Omnibus (GEO) and The Cancer Genome Atlas (TCGA) databases and meanwhile, we collected 230 immune related signatures by searching literatures. Single sample gene set enrichment analysis was performed on 230 signatures, and the normalized enrichment score of each patient was calculated. Then, the Immune Related Prognosis Score (IRPS) was constructed based on normalized enrichment scores. Finally, an extensive analysis was performed to explore the relationship between the IRPS and immune score, prognostic significance, microsatellite status, immunogenomic factors, cancer genotype and potential immune escape mechanism.

Results: We found that the IRPS can reflect the immune infiltration status of colorectal cancer patients, and it is related to some important immunophenotypic factors, such as neoantigen load and Tumor Mutational Burden (TMB). Further analysis confirmed that patients with the low IRPS had a better response to immune checkpoint inhibitors.

Conclusion: Based on these results, we can conclude that the IRPS may be an available tool for the prediction of immunotherapy efficacy in colorectal cancer patients.

Keywords: Colorectal cancer; Immunotherapy; IRPS; TMB; Prediction; Efficacy

INTRODUCTION

The Colorectal Cancer (CRC) is one of the most common cancers in the world, and it is also one of the main causes of cancer related death. In 2020, the incidence of CRC ranks fifth worldwide and the mortality is top five in global cancer related death [1]. In China, CRC incidence is higher and CRC ranks second in all cancers. At the same time, CRC cancer is the fourth cancer-related cause of death [2]. At present, the treatment method of CRC includes surgery, chemotherapy, radiotherapy and immunotherapy. Immune Checkpoint Inhibitors (ICIs) are new therapeutic strategies, which targets immune checkpoint molecules, including Programmed Cell Death Protein-1 (PD-1), Programmed Cell Death Ligand Protein-1 (PD-L1) and Cytotoxic T-Lymphocyte-Associated Protein 4 (CTLA4) [3]. In 2017, pembrolizumab (anti-PD-1 antibody) and nivolumab (anti-PD1 antibody) were attained FDA approval for the treatment of metastatic CRC.

Correspondence to: GuiYu Wang, Department of Colorectal Surgery, The Second Affiliated Hospital of Harbin Medical University, Harbin, China, E-mail: guiywang@163.com;

Lei Yu , Department of Colorectal Surgery, The Second Affiliated Hospital of Harbin Medical University, Harbin, China, E-mail: allengl0601@163.com

Received: 24-Mar-2023, Manuscript No. IGOA-23-22341; **Editor assigned:** 28-Mar-2023, PreQC No. IGOA-23-22341 (PQ); **Reviewed:** 11-Apr-2023, QC No. IGOA-23-22341; **Revised:** 20-Jun-2023, Manuscript No. IGOA-23-22341 (R); **Published:** 28-Jun-2023, DOI: 10.35248/IGOA.23.8.199

Citation: Xiang J, Li J, Cheng X, Hu H, Yu L, Wang G (2023) Constructing the Immune Related Prognosis Score to Predict the Benefit of Immunotherapy in Colorectal Cancer. Immunogenet Open Access.8:199

The Tumor Microenvironment (TME) is composed of non-malignant cells, such as Cancer Associated Fibroblasts (CAFs), endothelial cells and pericytes constituting tumor vascular system, immune cells, stromal cells and Extra-Cellular Matrix (ECM), which forms complex interaction with tumor [4-6]. Among the immune cells, except for the common T cells and B cells, TME also includes other immune cells such as dendritic cells, neutrophil, macrophages, and cytotoxic cells, regulatory T cells (Treg), Myeloid Derived Suppressor Cells (MDSCs) and NK cells5. The immunosuppressive cells include mast cells, Treg cells, Myeloid-Derived-Suppressor Cells (MDSCs) and Tumor Associated Macrophages (TAMs) with tumor promoting phenotype. Anti-tumor immune cells of TME mainly comprise T cells, B cells, NK cells and cytotoxic cells [5,7-9]. As a major component of TME, the infiltration level of immune cells contributes to tumor progression and immunotherapeutic response. And the difference of immune cell infiltration level in TME leads to the difference in chemotherapy response in different tumor patients, especially immunotherapy.

In CRC, ICIs only responded to CRC with mismatch repair Deficient And Microsatellite Instability-High (DMMR–MSI-H) and it has no clinical benefit on Mismatch-Repair-Proficient and Microsatellite Instability-Low CRC (pMMR–MSI-L) or Microsatellite Stability (MSS) CRC [10,11]. Now, several reports have indicated that there is an association between the increase of mutation load and the treatment response of anti-CTLA4 antibody or anti-PD-1 antibody [12-14]. Studies have found that neo-antigen load is related to Tumor Mutation Burden (TMB), so neo-antigen load is also related to response [13,14]. Only a subset of CRC patients benefits from immunotherapy, the precise biomarkers to predict immunotherapy efficacy are needed. Therefore, it is essential to confirm biomarkers and screen the dominant populations of ICIs efficacy.

Here, we are committed to establishing an immune signature of CRC to analyze the relationship between immune activities, tumor microenvironment and cancer genotype of CRC. On the basis of these prognosis-related immune signatures, the Immune Related Prognosis Score (IRPS) for CRC was developed, which was found to be related to the overall survival and immuno-phenotypic factors of patients with CRC. Moreover, we found that the IRPS can predict the patient's response to immune checkpoint blockade.

MATERIALS AND METHODS

Datasets collection and processing

Gene expression profiles and clinical datasets of CRC were collected from Gene Expression Omnibus (GEO), The Cancer Genome Atlas (TCGA) and PubMed. At the same time, downloading the genomic data of TCGA CRC from the Pan-cancer Atlas (https://gdc.cancer.gov/about-data/publications/pancanatlas).

Downloading the raw Chronic Eosinophilic Leukemia (CEL) files generated by Affymetrix in the GEO. The function Robust Multichip Average (RMA) in "affy" of R package was used to process and standardize the CEL files generated by Affymetrix. For the expression value of same gene symbol, we take the gene with the largest expression value.

Finally, more than 1800 tumor samples were obtained from 6 cohorts. GSE39582, GSE17538 and GSE103479 cohorts were used as discovery datasets; At the same time, TCGA, GSE12945 and GSE106584 cohorts were used as validation datasets. The potential batch effect between multicenter datasets was removed by the combat function in the R package "sva" [15].

In addition, we obtained two immunotherapy related cancer cohorts (GSE78220 and IMvigor210) from the GEO database and literature [16]. Melanoma patients in the GSE78220 cohort received anti-PD1 antibody therapy. Bladder cancer patients in the IMvigor210 cohort were treated with inhibitors of PD-L1.

Acquirement of immune-related data

We collected 230 immune related signatures by reading the literatures. The main signatures include 68 gene sets derived from the work of Wolf et al. [17], 34 gene sets from Meta-map [18] ,32signatures were obtained from the ImmuneSigDB (Collection C7 of MSigDB, Broad Institute) [19], 25 signatures were obtained from Bindea [20], 10 oncogenic pathway signatures [21], NK cell related signature [22], Exhausted $CD8^+$T cells signatures [23], APMs gene sets [24] and 85 Th1/IFN-γ gene signature [25]. More details can be seen in supplementary.

Single sample gene set enrichment analysis and immune-related estimation

The single sample Gene Set Enrichment Analysis (ssGSEA) was performed by using R package "GSVA", and The Normalized Enrichment Scores (NES) of 230 immune related signatures in each CRC sample were calculated by ssGSEA.

The immune score, tumor purity, stromal score and ESTIMATE score of each CRC patient are calculated on the basis of the NES, which is accomplished by R package "estimate".

The immune-related prognostic score for colorectal cancer

R package "GSVA" was used to implement ssGSEA for the signature of each sample and calculated the NES so that evaluating the immune infiltration level of immune related signature. Univariate Cox proportional hazards regression model was used to assess the correlation between the NES and overall survival in each sample of 6 CRC cohorts. Then, the fixed effect model in R package "meta" was used to evaluate the overall Hazards Ratio (HR) and P-value.

Finally, the IRPS combined with discovery datasets and immune cell signatures was defined as:

$$IRPS = \sum_{i=1}^{k} NES_i - \sum_{j=1}^{m} NES_j$$

Among them, NESi is the standardized ssGSEA score of the ith immune signature with total HR less than 1, and NESj is the standardized ssGSEA score of the jth immune signature with total HR more than 1.

Statistical analysis

The heatmaps and other plots were drawn by the "pheatmap" and "ggplot2". The R package "forestplot" was used to plot the forest plot. The Kaplan-Meier method was used to assess overall survival curves, and the distinct between survival distributions were assessed with the two-sided log-rank test as implemented in the R package "survival". A modified drawing survival curve function "gsurvplot", as implemented in the R package "survminer", was used for drawing the Kaplan-Meier survival curves in this research. The univariable Cox proportional hazard model was conducted to assess the association between signatures and the patient's overall survival. All the statistical analyses were performed in R program, and the P-value <0.05 was considered statistically significant.

RESULTS

Construction of the IRPS and the IRPS reflected the immune infiltration status

In order to establish an immune prognostic scoring model related to immune infiltration level, we analyzed 230 immune related signatures. First, we performed ssGSEA on 230 immune related signatures in discovery datasets and calculated the NES for all immune related signatures in each patient. Next, the HRs of the NES in each patient was assessed by univariate Cox regression model, and a meta-analysis was performed on all immune related signatures to assess the overall prognosis. We finally identified 48 immune related signatures with significant prognostic value (HR<1 or HR>1, P<0.05). Among the 48 signatures, the HR values of 31 signatures was less than 1, indicating that the higher the NES, the longer the survival time of patients; However, the HR values of the 17 signatures >1 indicates that the NES is high and the prognosis of patients is poor. Finally, we constructed IRPS based on the NES of 48 immune related signatures (Figure 1 and Table 1).

Among the 48 immune related signatures, the infiltration levels of immune cells (T cells, Th1 cells, Tcm cells, Tem cells, NK cells and mast cells) plays a role for the prognosis of patients as shown in Figure 2A. It is well known that T cells and NK cells play an immune promoting role in the anti-tumor process [7-9]. We observed that the IRPS was significantly negatively related to immune promoting cells, such as T cells and NK cells; however, the IRPS showed positive correlation with immunosuppressive cells (Th1 cells, Tcm cells, Tem cells and mast cells) as shown in Figures 2B and 2C. We observed similar results in the validation dataset. These results show that the IRPS may play an immunosuppressive role in the anti-tumor process.

In addition, the level of immune infiltration also plays an important role in the anti-tumor process. Therefore, we calculated the immune infiltration score for each sample, including ESTIMATE score, immune score, stromal score, and tumor purity. By analyzing the correlation between the IRPS and immune infiltration score, we observed that the IRPS was significantly positively correlated with ESTIMATE score, immune score and stromal score. On the contrary, the IRPS was negatively correlated with tumor purity as shown in Figures 2D and 2E.

We observed that the IRPS constructed by the NES according to immune related signatures have immune inhibiting effects in the process of anti-tumor immunity and can reflect the level of immune infiltration in CRC patients (Figures 2A-2E).

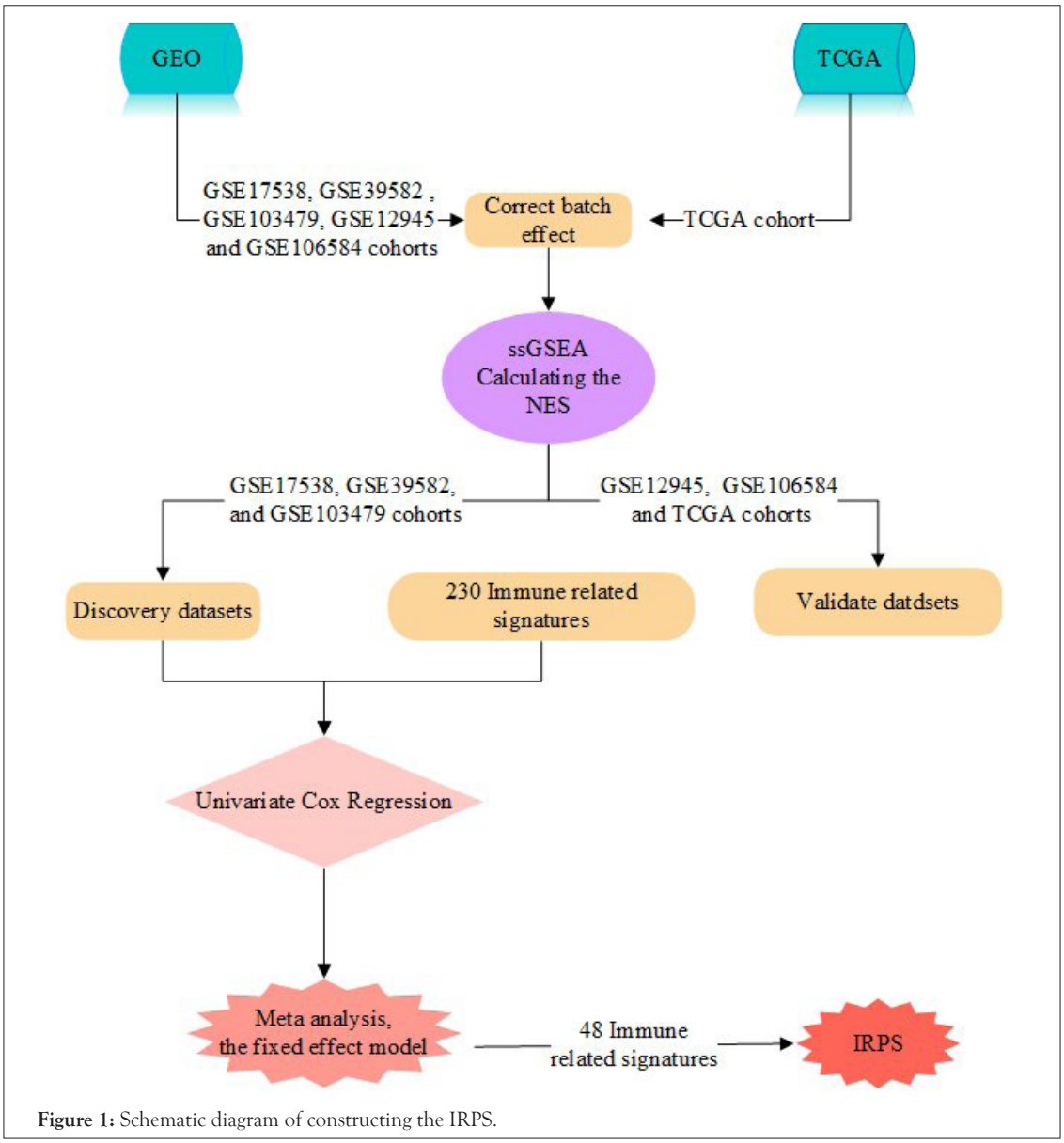

Figure 1: Schematic diagram of constructing the IRPS.

Table 1: Immune related signature.

Signature	HR	CI	P value
EP_BLOOD_VESS_DEVEL_DN_IN_R	0.3196	0.2177-0.4694	<0.0001
CD103pos_CD103neg_ratio	0.3589	0.2268-0.5679	<0.0001
WOUNDING_UP_IN_MAPKi_aPDL1_NR	0.441	0.3386-0.5745	<0.0001
C7_Atom_21	0.4603	0.3448-0.6145	<0.0001
Tcm_cells	0.4644	0.3644-0.5919	<0.0001
MAPKi_INDUCED_ANGIOGENESIS	0.4861	0.3784-0.6244	<0.0001
Tem_cells	0.4965	0.3794-0.6497	<0.0001
Mast_cells	0.4993	0.3819-0.6527	<0.0001
Th1_cells	0.5035	0.3817-0.6642	<0.0001
HYPOXIA_UP_IN_MAPKi_aPDL1_NR	0.5056	0.3759-0.6802	<0.0001
TGFβ_pathway	0.5099	0.3762-0.6909	<0.0001
DTPP_REG_CELL_PROLIF_UP	0.5108	0.3959-0.6591	<0.0001
Core_Inhibition	0.5203	0.4194-0.6455	<0.0001
DTP_BLOOD_VESS_DEVEL_UP	0.5261	0.4094-0.6761	<0.0001
CD68	0.5409	0.4319-0.6775	<0.0001
Immunosupppressive_core_pathways	0.5543	0.4433-0.6930	<0.0001
MCD3_CD8	0.5631	0.4490-0.7062	<0.0001
Danger_signal_pathways	0.5644	0.4341-0.7337	< 0.0001
GRANS_PCA	0.5665	0.4443-0.7223	< 0.0001
PH_RESP_TO_WOUNDING_DN_IN_R	0.5756	0.4656-0.7116	<0.0001
PH_BLOOD_VESS_DEVEL_DN_IN_R	0.5864	0.4630-0.7427	<0.0001
C7_Atom_10	0.5876	0.4554-0.7582	<0.0001
PLX2D_CELL_ADHESION_UP	0.5914	0.4770-0.7332	<0.0001
TGFB_PCA	0.5976	0.4743-0.7530	<0.0001
C7_Atom_22	0.602	0.4719-0.7679	<0.0001
C7_Atom_11	0.6041	0.4804-0.7595	<0.0001
MAPKR_BLOOD_VESS_DEVEL_UP	0.6042	0.4679-0.7802	0.0001
NK_cells	0.6214	0.4978-0.7756	<0.0001
HIPPO_pathway	0.6256	0.5002-0.7825	<0.0001
Core_Activation	0.6324	0.4887-0.8183	0.0005
G_CYTH4	0.6354	0.5036-0.8017	0.0001
CD8A	1.2367	1.0992-1.5306	0.0051
NK_cell	1.2543	1.0120-1.5547	0.0386
T_cells	1.5277	1.2134-1.9234	0.0003
CSR_Activated	1.6003	1.2637-2.0267	<0.0001
NRF2_pathway	1.6136	1.2972-2.0071	<0.0001
G_CD3E	1.6849	1.3133-2.1617	<0.0001
T_cell	1.6982	1.2935-2.2295	0.0001
Tcell_receptors	1.7123	1.3707-2.1389	<0.0001
C7_Atom_15	1.7735	1.3691-2.2975	<0.0001
Module5_TcellBcell	1.8306	1.4016-2.3910	<0.0001
TIS_signature	1.8336	1.4199-2.3679	<0.0001
TAMsurr_TcClassII_ratio	1.8961	1.4248-2.5232	<0.0001
T_helper_cells	1.9174	1.4740-2.4941	<0.0001
APMS	2.0022	1.5968-2.5105	<0.0001
IL8	2.2732	1.7192-3.0057	<0.0001
ICR	2.3475	1.8145-3.0370	<0.0001
ICR_ACT	2.4897	1.9175-3.2326	<0.0001

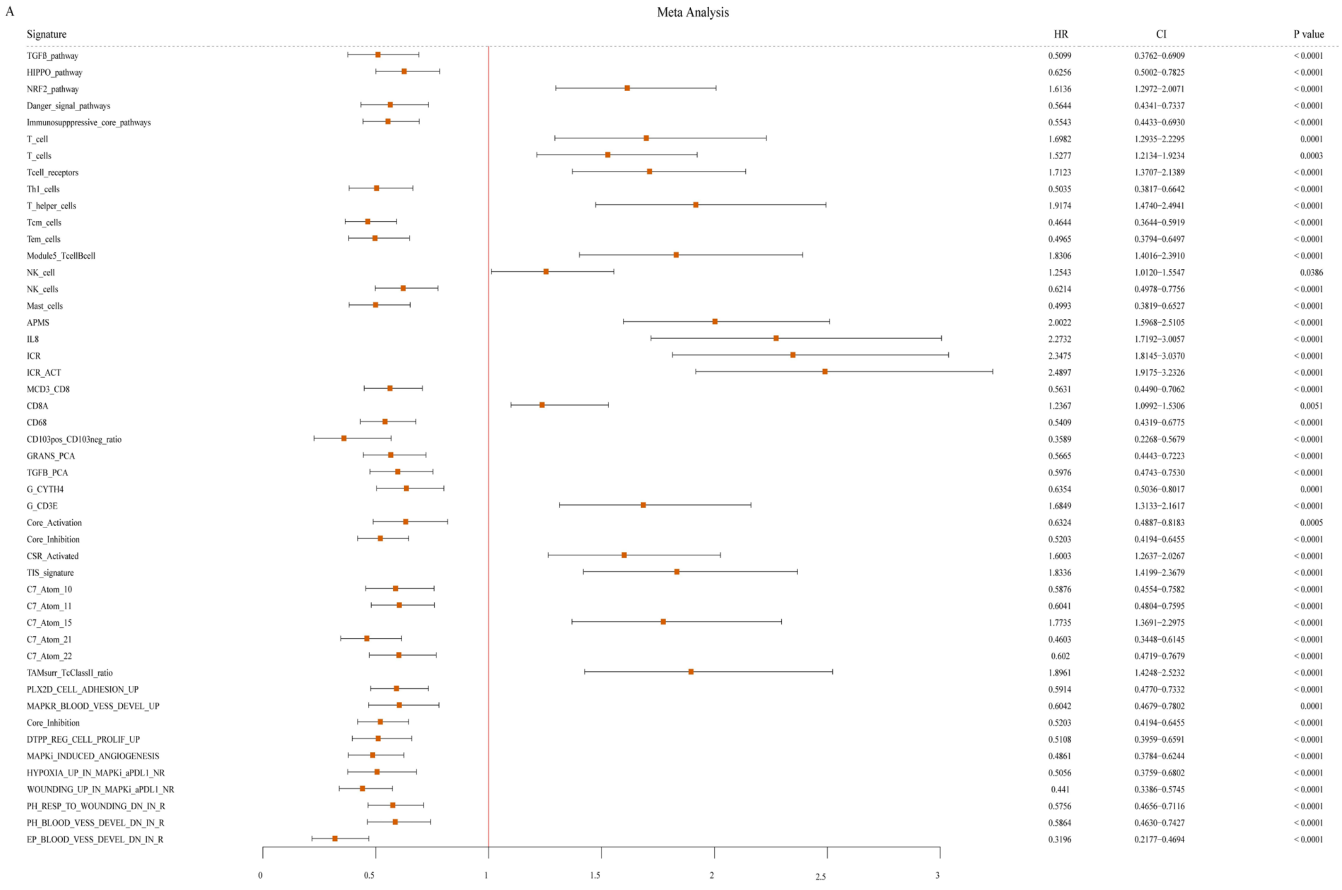
A
Meta Analysis
Signature
HR
CI
P value
TGFB_pathway 0.5099 0.3762−0.6909 < 0.0001
HIPPO_pathway 0.6256 0.5002−0.7825 < 0.0001
NRF2_pathway 1.6136 1.2972−2.0071 < 0.0001
Danger_signal_pathways 0.5644 0.4341−0.7337 < 0.0001
Immunosupppressive_core_pathways 0.5543 0.4433−0.6930 < 0.0001
T_cell 1.6982 1.2935−2.2295 0.0001
T_cells 1.5277 1.2134−1.9234 0.0003
Tcell_receptors 1.7123 1.3707−2.1389 < 0.0001
Th1_cells 0.5035 0.3817−0.6642 < 0.0001
T_helper_cells 1.9174 1.4740−2.4941 < 0.0001
Tcm_cells 0.4644 0.3644−0.5919 < 0.0001
Tem_cells 0.4965 0.3794−0.6497 < 0.0001
Module5_TcellBcell 1.8306 1.4016−2.3910 < 0.0001
NK_cell 1.2543 1.0120−1.5547 0.0386
NK_cells 0.6214 0.4978−0.7756 < 0.0001
Mast_cells 0.4993 0.3819−0.6527 < 0.0001
APMS 2.0022 1.5968−2.5105 < 0.0001
IL8 2.2732 1.7192−3.0057 < 0.0001
ICR 2.3475 1.8145−3.0370 < 0.0001
ICR_ACT 2.4897 1.9175−3.2326 < 0.0001
MCD3_CD8 0.5631 0.4490−0.7062 < 0.0001
CD8A 1.2367 1.0992−1.5306 0.0051
CD68 0.5409 0.4319−0.6775 < 0.0001
CD103pos_CD103neg_ratio 0.3589 0.2268−0.5679 < 0.0001
GRANS_PCA 0.5665 0.4443−0.7223 < 0.0001
TGFB_PCA 0.5976 0.4743−0.7530 < 0.0001
G_CYTH4 0.6354 0.5036−0.8017 0.0001
G_CD3E 1.6849 1.3133−2.1617 < 0.0001
Core_Activation 0.6324 0.4887−0.8183 0.0005
Core_Inhibition 0.5203 0.4194−0.6455 < 0.0001
CSR_Activated 1.6003 1.2637−2.0267 < 0.0001
TIS_signature 1.8336 1.4199−2.3679 < 0.0001
C7_Atom_10 0.5876 0.4554−0.7582 < 0.0001
C7_Atom_11 0.6041 0.4804−0.7595 < 0.0001
C7_Atom_15 1.7735 1.3691−2.2975 < 0.0001
C7_Atom_21 0.4603 0.3448−0.6145 < 0.0001
C7_Atom_22 0.602 0.4719−0.7679 < 0.0001
TAMsurr_TcClassII_ratio 1.8961 1.4248−2.5232 < 0.0001
PLX2D_CELL_ADHESION_UP 0.5914 0.4770−0.7332 < 0.0001
MAPKR_BLOOD_VESS_DEVEL_UP 0.6042 0.4679−0.7802 0.0001
Core_Inhibition 0.5203 0.4194−0.6455 < 0.0001
DTPP_REG_CELL_PROLIF_UP 0.5108 0.3959−0.6591 < 0.0001
MAPKi_INDUCED_ANGIOGENESIS 0.4861 0.3784−0.6244 < 0.0001
HYPOXIA_UP_IN_MAPKi_aPDL1_NR 0.5056 0.3759−0.6802 < 0.0001
WOUNDING_UP_IN_MAPKi_aPDL1_NR 0.441 0.3386−0.5745 < 0.0001
PH_RESP_TO_WOUNDING_DN_IN_R 0.5756 0.4656−0.7116 < 0.0001
PH_BLOOD_VESS_DEVEL_DN_IN_R 0.5864 0.4630−0.7427 < 0.0001
EP_BLOOD_VESS_DEVEL_DN_IN_R 0.3196 0.2177−0.4694 < 0.0001
0
0.5
1
1.5
2
2.5
3
B
GSE39582
IRPS
TGFß_pathway
HIPPO_pathway
NRF2_pathway
Danger_signal_pathways
Immunosupppressive_core_pathways
T_cell
T_cells
Tcell_receptors
Th1_cells
T_helper_cells
Tcm_cells
Tem_cells
Module5_TcellBcell
NK_cell
NK_cells
Mast_cells
APMS
IL8
ICR
ICR_ACT
MCD3_CD8
CD8A
CD68
CD103pos_CD103neg_ratio
GRANS_PCA
TGFB_PCA
G_CYTH4
G_CD3E
Core_Activation
Core_Inhibition
CSR_Activated
TIS_signature
C7_Atom_10
C7_Atom_11
C7_Atom_15
C7_Atom_21
C7_Atom_22
TAMsurr_TcClassII_ratio
PLX2D_CELL_ADHESION_UP
MAPKR_BLOOD_VESS_DEVEL_UP
DTP_BLOOD_VESS_DEVEL_UP
DTPP_REG_CELL_PROLIF_UP
MAPKi_INDUCED_ANGIOGENESIS
HYPOXIA_UP_IN_MAPKi_aPDL1_NR
WOUNDING_UP_IN_MAPKi_aPDL1_NR
PH_RESP_TO_WOUNDING_DN_IN_R
PH_BLOOD_VESS_DEVEL_DN_IN_R
EP_BLOOD_VESS_DEVEL_DN_IN_R
1
0.8
0.6
0.4
0.2
0
−0.2
−0.4

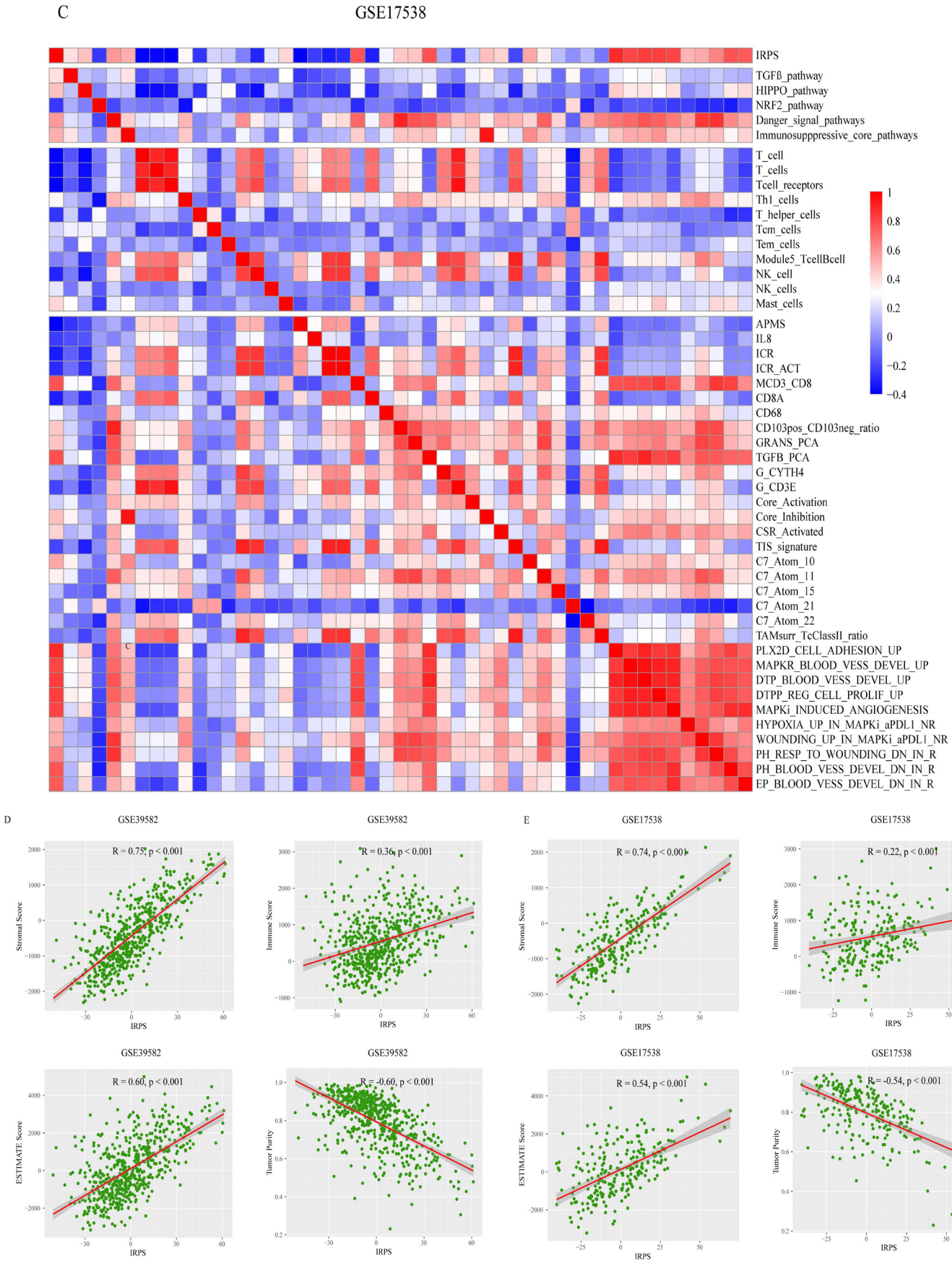

Figure 2: Construction of the IRPS and exploration of immune infiltration level. (A) The forest plot of immune related signatures; (B and C) Correlation heatmap between immune infiltrating cells and the IRPS in GSE39582 and GSE17538 respectively; (D and E) scatter plot of the IRPS and immune infiltration score in GSE39582 and GSE17538 respectively.

Relationship between the IRPS and microsatellite status in colorectal cancer

We divided all patients into the high IRPS group and the low IRPS group according to the best cut-off of the IRPS. Subsequently, we compared the overall survival of patients in different the IRPS groups. We found that there was a significant difference in overall survival between the high IRPS group and the low IRPS group by survival analysis of the discovery datasets. In GSE39582 and GSE17538 cohorts, the overall survival time of patients in the low IRPS group was significantly longer than that in the high IRPS group as shown in Figure 3A; however, in the GSE103479 cohort, we observed the opposite result, although the analysis results were not statistically significant. Meanwhile, we also carried out survival analysis on the validation datasets, we observed the similar result in the three validate cohorts, that is, the overall survival time of patients in the low IRPS group was significantly longer. This suggests that the IRPS may act as a risk factor in CRC patients.

We know that the microsatellite status of CRC patients is an important factor affecting their prognosis and affects the patient's response to immunotherapy. To further clarify the impact of the IRPS on CRC patients, we performed an association analysis between the IRPS and microsatellite status. In our cohorts, only the GSE39582 and TCGA cohorts recorded microsatellite status information of patients, so we only further analyzed these two cohorts. Classifying CRC patients into Medical Student Section (MSS) subtype and Microsatellite Instability (MSI) subtype according to the microsatellite status of each patient. We first performed survival analysis on patients in different subtypes. This is obvious, in both the discovery and validation dataset, patients in the low IRPS group had a longer survival time as show in Figures 3B and 3C. In the TCGA cohort, the survival analysis results of MSI subtype patients were not statistically significant, which may be due to the small number of samples. Then, we found the IRPS is significantly lower in patients with MSI subtype as show in Figure 3D. We further analyzed the distinction between the high IRPS and the low IRPS in the different microsatellite status. We can view that there is significant difference between the high IRPS group and the low IRPS group in two microsatellite status subtypes, and the IRPS is significantly lower in patients with MSI subtype as shown in Figures 3E and 3F.

These results prove that the IRPS is a prognostic factor of CRC. At the same time, by analyzing the differences of the IRPS in patients with different microsatellite status, we find that the level of the IRPS may potentially reflect the patient's response to immunotherapy in different microsatellite status (Figures 3A-3F).

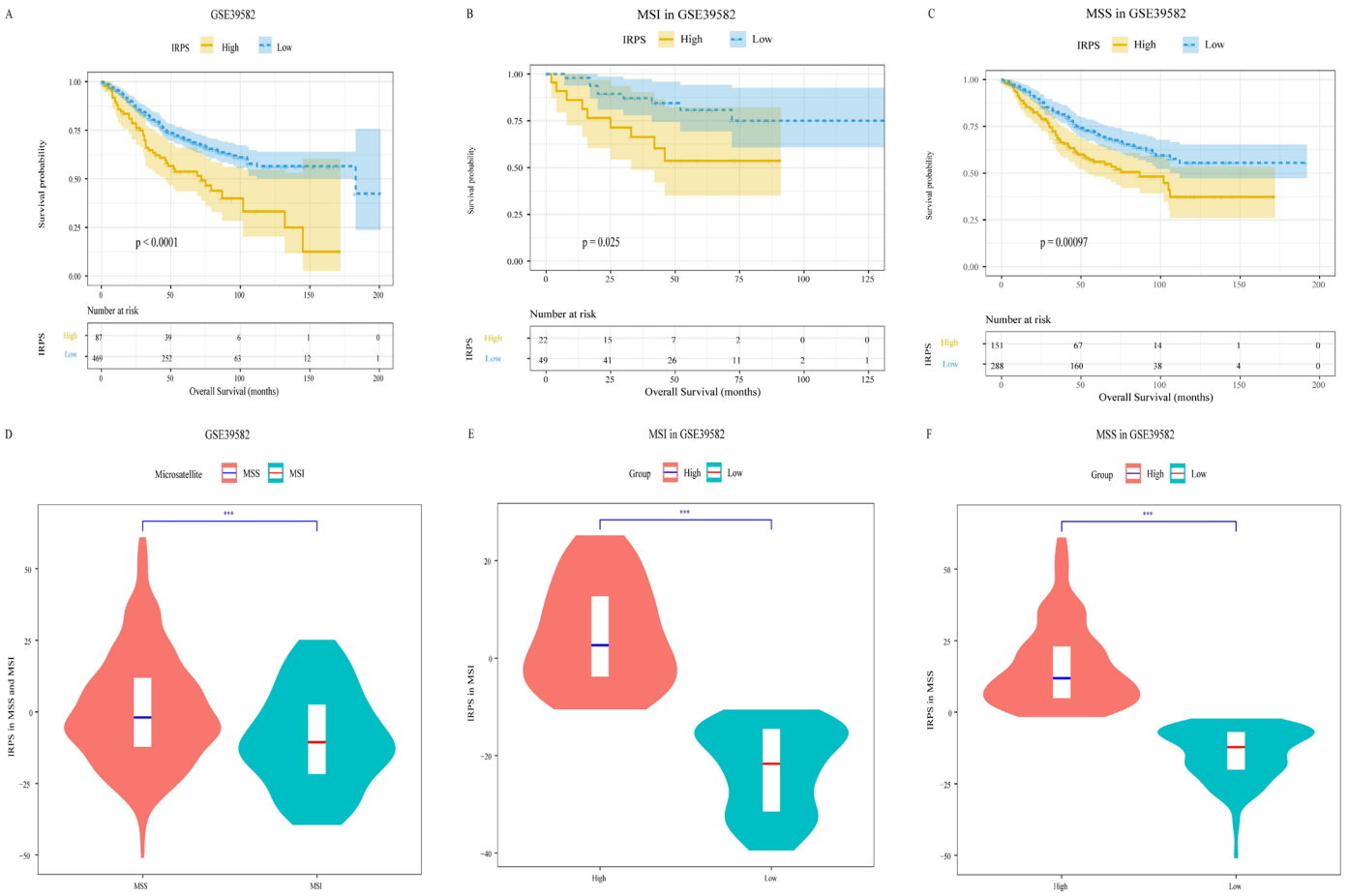

Figure 3: Stratified analysis of CRC and the IRPS. (A) The survival analysis of the IRPS in GSE39582; (B and C) the survival analysis of the MSI and MSS subtypes; (D) the differential analysis of the NES in the MSS and MSI subtypes; (E) the differential analysis of NES values in MSI subtype; (F) the differential analysis of the NES in MSS subtype. **Note:** Figure (A) IRPS in GSE39582 (—) High, (- -) Low; Figure (B) MSI in GSE39582 IRPS (—) High, (- -) Low; MSS in GSE39582 IRPS (—) High, (- -) Low; Figure (D) GSE39582 Microsatellite (▭) MSS, (▭) MSI; Figure (E) MSI in GSE39582 Group (▭) High, (▭) Low; Figure (F) MSS in GSE39582 Group (▭) High, (▭) Low.

Association between innate immune escape mechanism and the IRPS in colorectal cancer

The intrinsic immune escape mechanism of tumor to immunotherapy mainly has two aspects, immunogenicity and immune checkpoint molecular expression [26]. Several potential prognostic factors, including TMB, Homologous Recombination Deficient (HRD), neo-antigen load, Loss Of Heterozygosity (LOH), Copy Number Variation (CNV) and Single Nucleotide Variation (SNV), determined tumor immunogenicity. In order to explore the effect of the IRPS on innate immune escape of CRC, we analyzed the relationship between the IRPS and tumor immunogenicity of CRC. In all our cohorts, the validation dataset TCGA cohort has complete genomic information, so we used the TCGA cohort for further analysis.

By comparing the differences of these potential prognosis factors between the high IRPS group and the low IRPS group, we found the prognostic factors CNV, LOH and HRD were higher in the low IRPS subtype than in the high IRPS subtype as shown in Figures 4A-4H. Opposite, the median values of prognostic factors immunogenic indel, indel, TMB, neo-antigen load and SNV tend to be highly expressed in the high IRPS subtype as shown in Figures 4B-4G. We further analyzed the correlation between the IRPS and prognostic factors. Unsurprisingly, the IRPS was negatively correlated with CNV, LOH and HRD as shown in Figures 5A-5H. Simultaneously, the IRPS was positively correlated with immunogenic indel, indel, TMB, neo-antigen load and SNV as shown in Figures 5B-5G.

As a prognostic factor of MSI patients, MSI patients with high TMB are effective for immunotherapy. Given the significant differential expression of the IRPS in MSI tumors as shown in Figure 3E and the positive correlation between the IRPS and TMB as shown in Figure 4E, we speculated that genomic changes in tumors might remodel the immune phenotype (Figures 4A-4H and Figures 5A-5G).

Exploring relationship between the IRPS and genomic alterations in colorectal cancer

To verify whether the immune phenotype is remodeled by genomic alterations of the tumor, we analyzed the associations between the IRPS and somatic mutations in the TCGA cohort. Firstly, we calculated the somatic mutation frequency of each gene in the cohort and visualized the somatic mutation frequency of the top 35 genes. We observed that the genes with the highest somatic mutation frequency in CRC were Antigen-Presenting Cell (APC) and TP53, followed by Kirsten Rat Sarcoma Viral Oncogene Homolog (KRAS) and Phosphatidylinositol-4,5-Bisphosphate 3-Kinase Catalytic Subunit Alpha (PIK3CA). These genes with high mutation frequency are common in some carcinogenic pathways, including cell cycle pathway, Hippo signaling, MYC signaling, Neurogenic Locus Notch Homolog Protein (NOTCH) signaling, oxidative stress response / Nuclear Factor Erythroid 2 (NRF2), PI-3-Kinase signaling, Receptor-Tyrosine Kinase (RTK) / Renin-Angiotensin-System (RAS) / Mitogen-Activated Protein Kinase (MAPK) signaling, Transforming Growth Factor (TGF-β) signaling, TP53 pathway and Wingless-Related Integration Site (WNT) /β-catenin signaling21.

Subsequently, we discussed the difference of NES of 10 oncogenic pathways between the high IRPS and the low IRPS subtypes in TCGA cohort as shown in Figures 6A-6L. It is obvious that the NES of most of the 10 carcinogenic pathways are higher in low IRPS subtypes, in particular, Hippo signaling, MYC signaling, oxidative stress response/NRF2, PI-3-Kinase signaling and TP53 pathway. Only the NES of cell cycle pathway and NOTCH signaling is higher in the high IRPS subtype. This seems to verify that somatic mutations in common carcinogenic pathways can affect the immuno-phenotype of patients with CRC (Figures 6A-6L).

The IRPS could predict the immunotherapeutic benefit

Based on the results of the previous analysis, it is suggested that there may be a potential association between the IRPS and immunotherapy of CRC, so we further analyzed the immunotherapeutic benefits of the IRPS in CRC. For doing this, we need to obtain the datasets of CRC immunotherapy firstly, but after searching the published CRC immunotherapy datasets, there is no suitable cohorts related to CRC immunotherapy. Instead, we used melanoma and bladder cancer immunotherapy cohort (GSE78220 and IMvigor210) to test the immunotherapeutic benefits of the IRPS.

Taking the best cut-off value of the IRPS as the cut-off value, patients in GSE78220 and IMvigor210 cohorts were divided into the high IRPS subtype and the low IRPS subtype. Patients in the low IRPS subtype had longer overall survival compared with patients in the higher IRPS subtype in the GSE78220 cohort (P-value=0.0079) as shown in Figures 7A-7J and IMvigor210 cohort (P-value=0.0012) as shown in Figure 7E. The violin diagram showed that the IRPS of patients who responded to immunotherapy decreased significantly compared with patients who did not respond to immunotherapy as shown in Figures 7B and 7F. The association between immunotherapy response and existing immune activity was analyzed by using the information about immunotherapy response in two immunotherapy cohorts we collected. We observed that patients in the low IRPS subtype responded better to immunotherapy than patients in the higher IRPS subtype as shown in Figures 7C and 7G. Finally, the waterfall plot of two immunotherapy datasets illustrates more patients with CR/PR for the immunotherapy have lower the IRPS value than PD/SD patients for the immunotherapy as shown in Figures 7D and 7H.

In the cohort of GSE78220 and IMvigor210, the IRPS significantly related to the efficacy of immunotherapy was evaluated by predictive model. By using the IRPS as input parameter of Support Vector Machine (SVM), support vector machine is implemented in R software package “e1071”. Radial Basis Function (RBF) is selected as the kernel function of support vector machine. The grid search is used to optimize the penalty parameter C and kernel coefficient gamma of support vector machine. The IRPS subtype of patients is used as the prediction target of the classifier. In the test, the overall accuracy of GSE78220 and IMvigor210 cohort in predicting patients' immunotherapy response was 0.929 and 0.975, respectively as show in Figures 7I and 7J. The predictive power of the two immunotherapy cohorts clearly shows that the IRPS is a predictive biomarker of immunotherapy benefits (Figures 7A-7J).

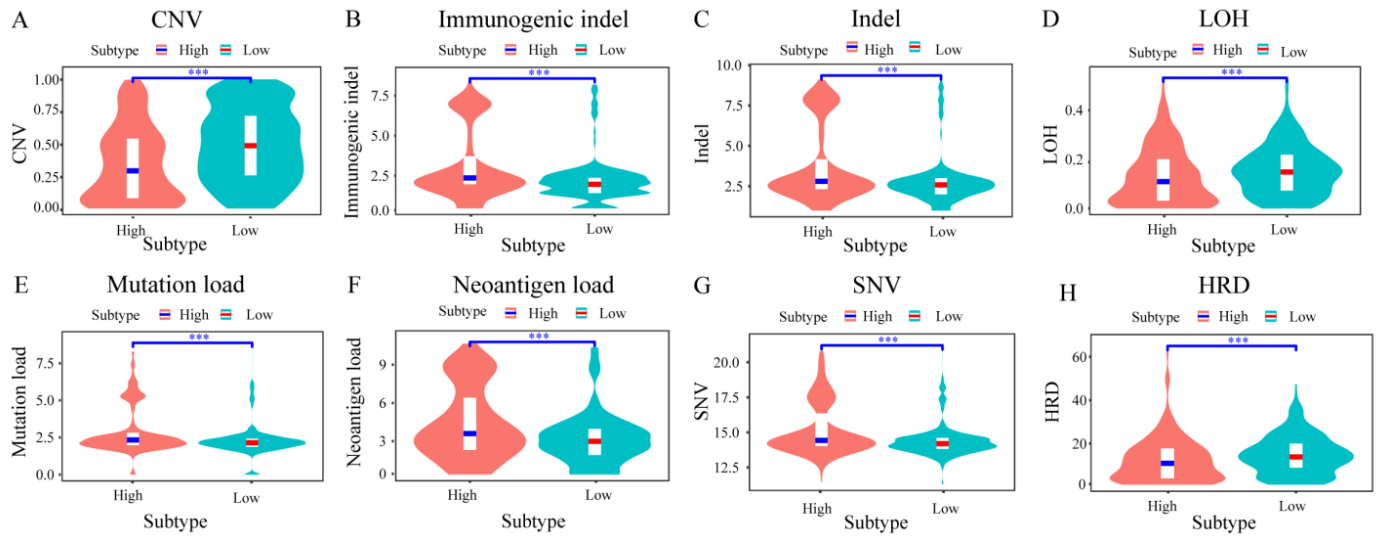

Figure 4: Immunogenicity analysis violin plot of CRC in TCGA. (A-H) The violin plot of immunogenicity in high and low IRPS subtypes, CNV, immunogenic indel, indel, LOH, mutation load, Neo-antigen load, SNV and HRD, respectively. **Note:** (🟥) High, (🟦) Low.

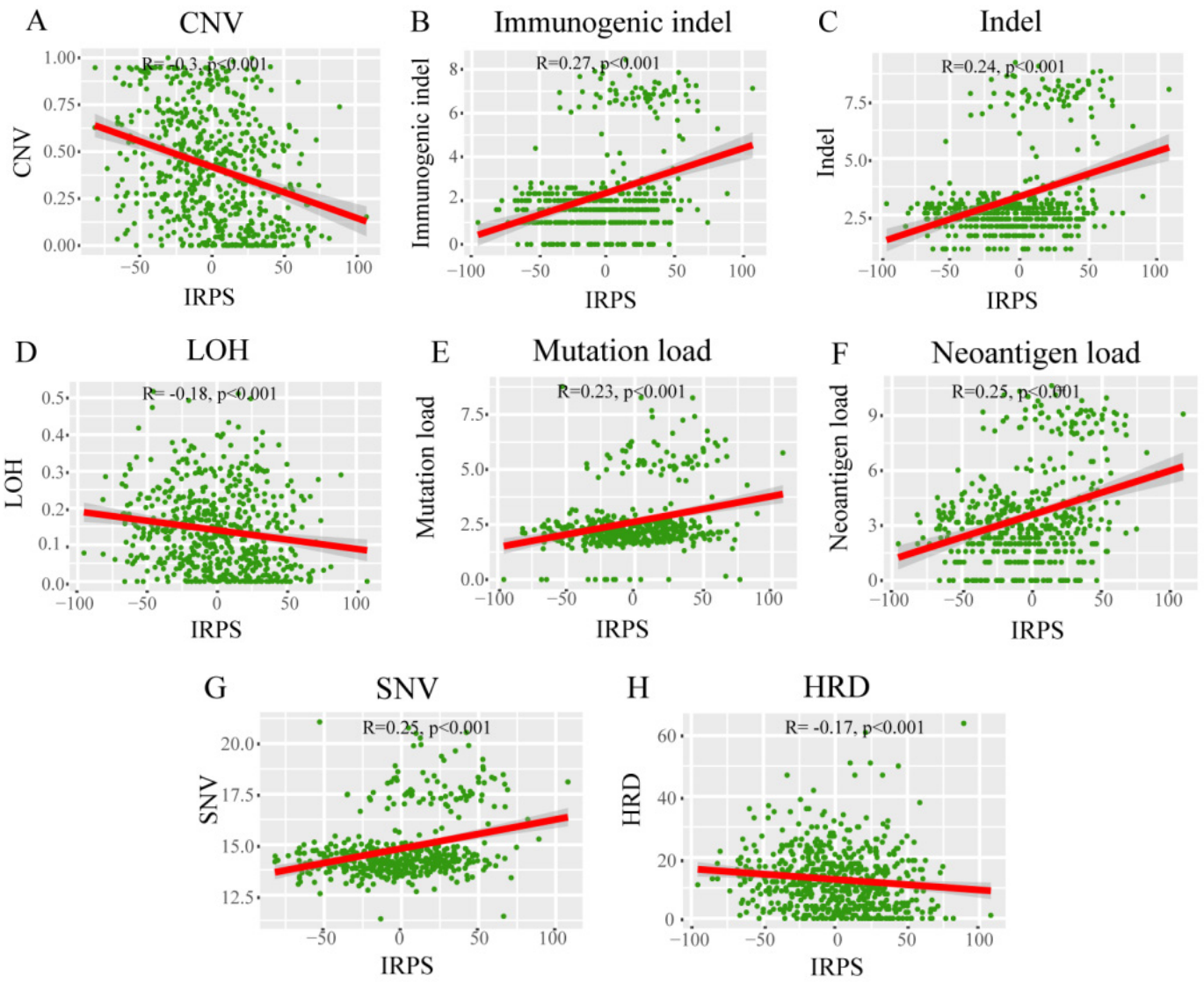

Figure 5: Immunogenicity analysis scatter plot of CRC in TCGA. (A-H) The violin plot of immunogenicity in the high and low IRPS subtypes, CNV, immunogenic indel, indel, LOH, mutation load, Neo-antigen load, SNV and HRD, respectively.

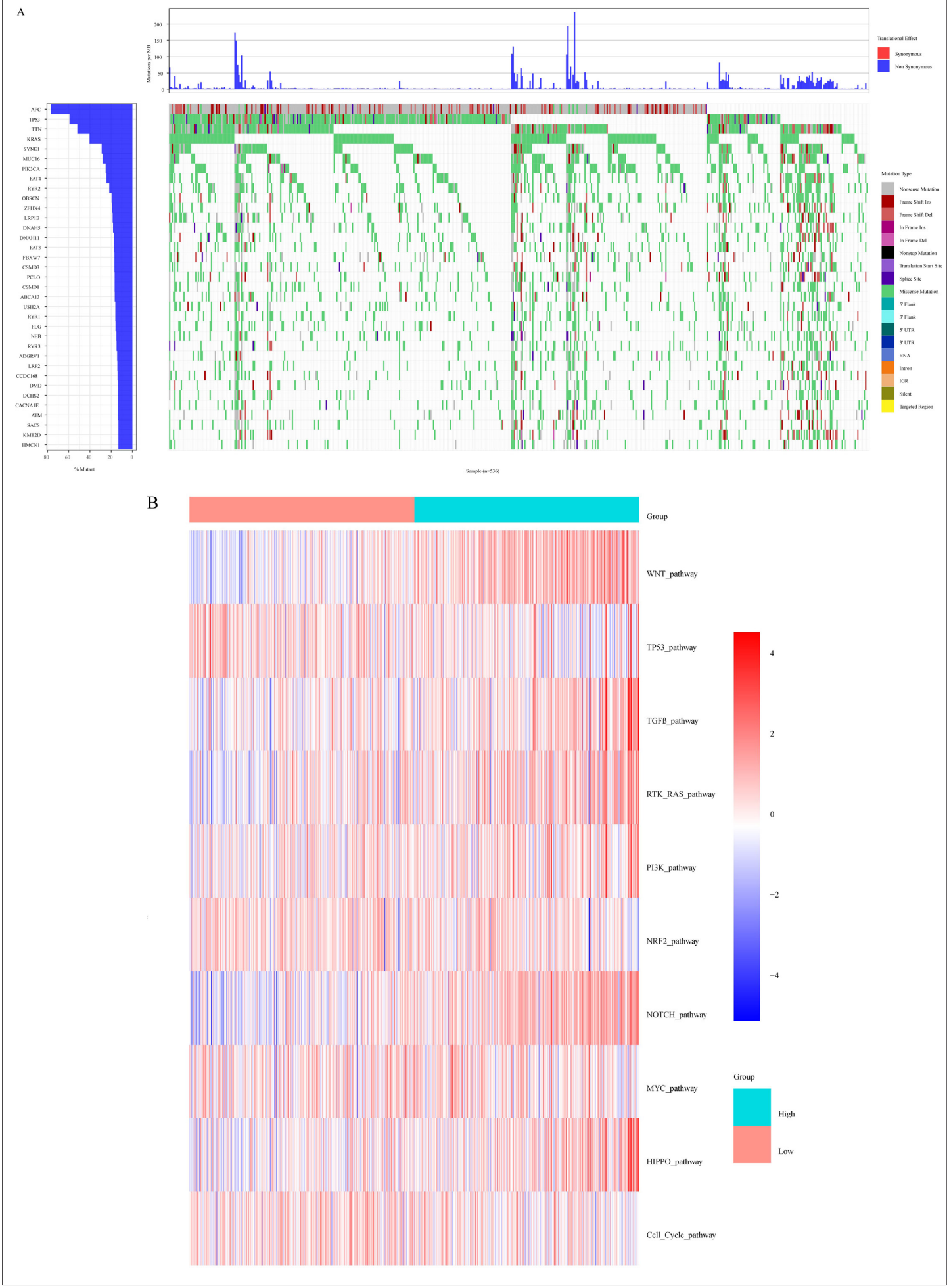
A
Mutations per MB
200
150
100
50
0
Translational Effect
Synonymous
Non Synonymous
APC
TP53
TTN
KRAS
SYNE1
MUC16
PIK3CA
FAT4
RYR2
OBSCN
ZFHX4
LRP1B
DNAH5
DNAH11
FAT3
FBXW7
CSMD3
PCLO
CSMD1
ABCA13
USH2A
RYR1
FLG
NEB
RYR3
ADGRV1
LRP2
CCDC168
DMD
DCHS2
CACNA1E
ATM
SACS
KMT2D
HMCN1
80
60
40
20
0
% Mutant
Sample (n=536)
Mutation Type
Nonsense Mutation
Frame Shift Ins
Frame Shift Del
In Frame Ins
In Frame Del
Nonstop Mutation
Translation Start Site
Splice Site
Missense Mutation
5' Flank
3' Flank
5' UTR
3' UTR
RNA
Intron
IGR
Silent
Targeted Region
B
Group
WNT_pathway
TP53_pathway
TGFß_pathway
RTK_RAS_pathway
PI3K_pathway
NRF2_pathway
NOTCH_pathway
MYC_pathway
HIPPO_pathway
Cell_Cycle_pathway
4
2
0
−2
−4
Group
High
Low

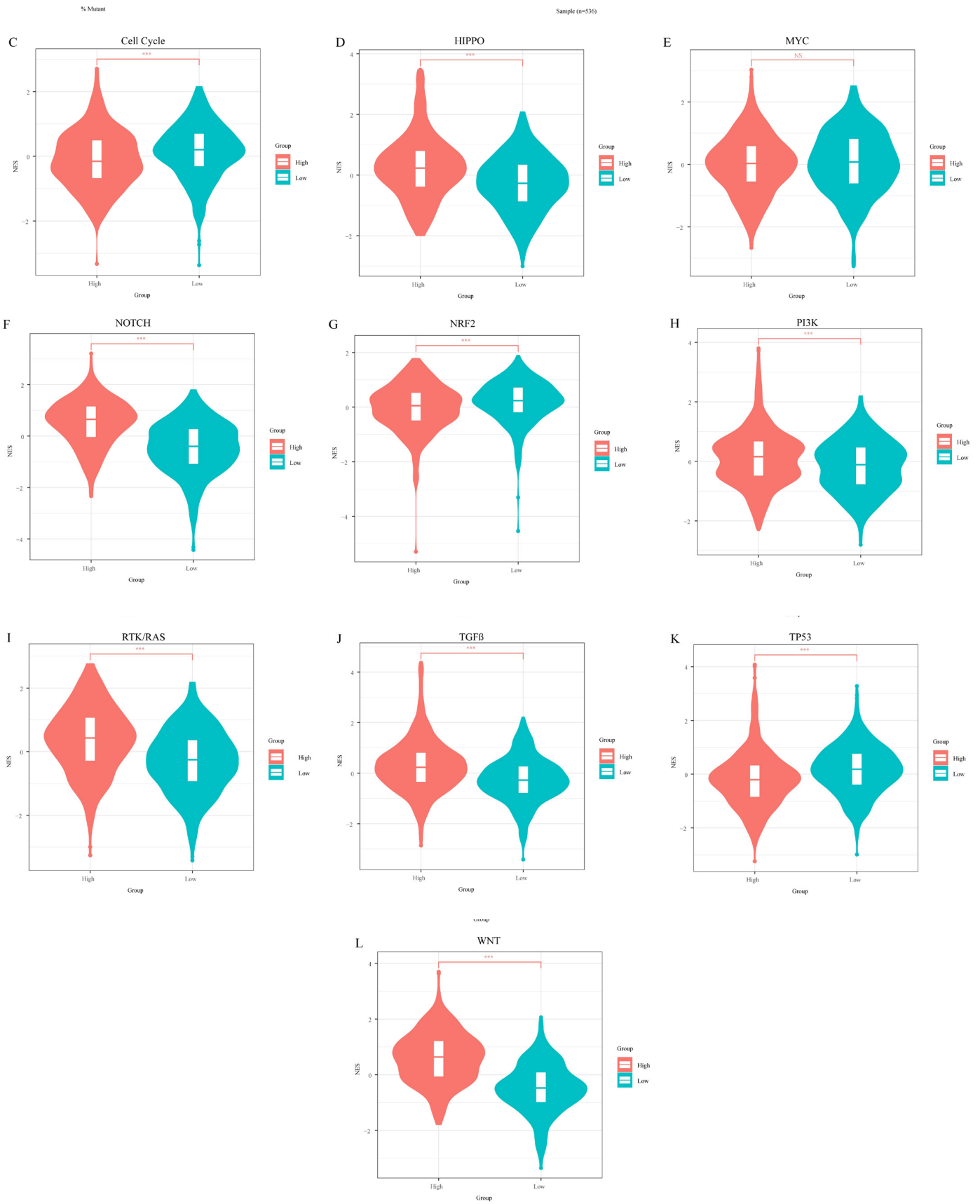

Figure 6: Analysis of genomic alteration in TCGA cohort. (A) Oncoplot of gene mutation frequency of top35 genes; (B) heatmaps of 10 oncogenic pathway NES values in different IRPS subtype; (C) stratified analysis of 10 oncogenic pathway NES values in the high and low IRPS subtypes. **Note:** Figure (A) (■) Synonymous, (■) Non synonymous; Figure (B) (■) High, (■) Low; Figures (C-L) (■) High, (■) Low

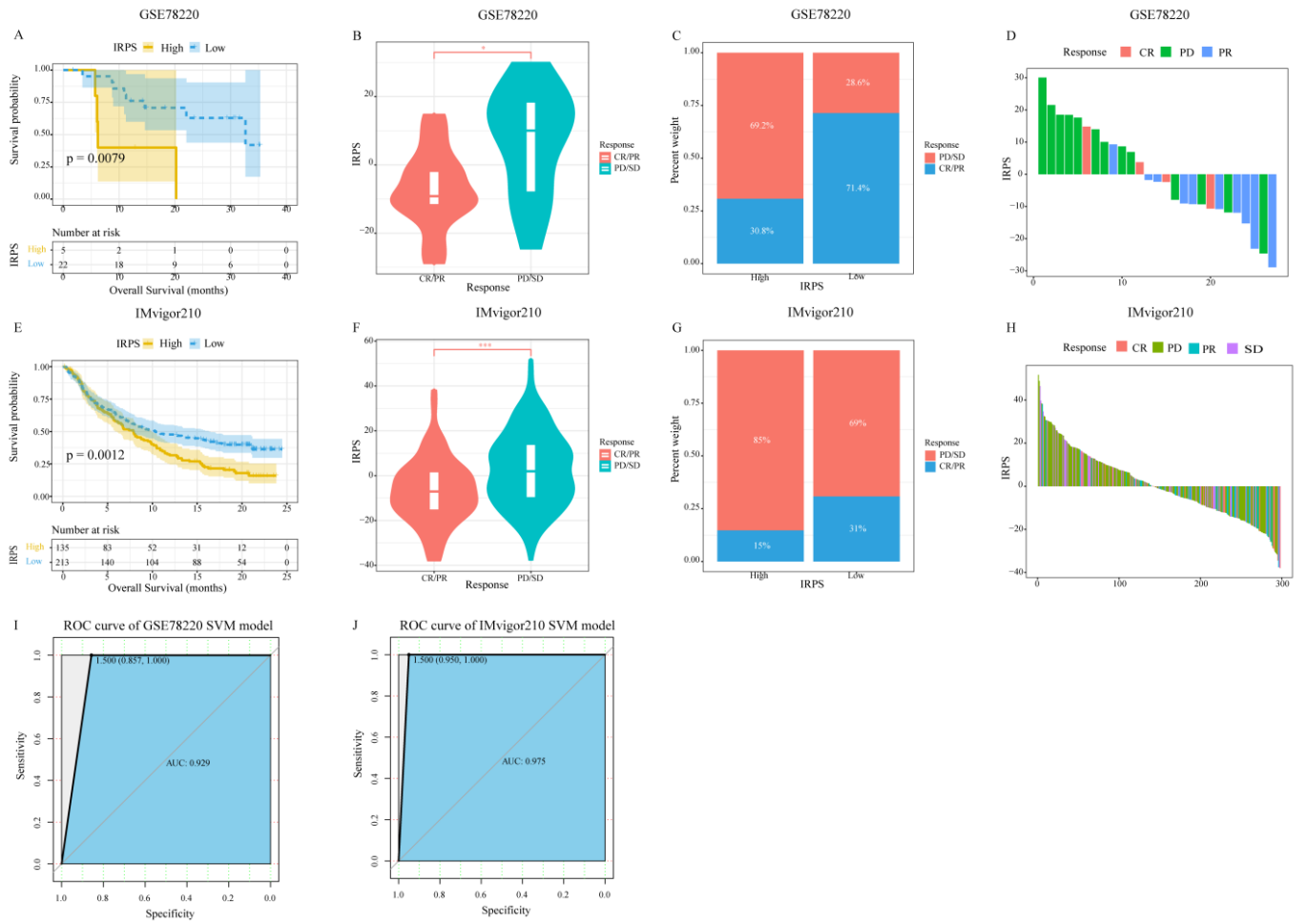

Figure 7: Efficacy analysis of the IRPS in GSE78220 and IMvigor210 cohorts. (A,E) overall survival curves for patients with the high and low IRPS subtypes for GSE78220 and IMvigor210 cohorts respectively; (B,F) the violin plots shown the distribution of the IRPS for patients with different immunotherapy response in GSE78220 and IMvigor210 cohorts; (C,G) bar graph illustrated the CR/PR and SD/PD to immunotherapy in the high and low IRPS subtypes in GSE78220 and IMvigor210 cohorts, respectively; (D,G) waterfall plot illustrated the IRPS with different immunotherapy efficacy in GSE78220 and IMvigor210 cohorts, respectively; (I) Prediction efficacy of the IRPS in immunotherapy cohort GSE78220; (J) Prediction efficacy of the IRPS in immunotherapy cohort IMvigor210. **Note:** Figures (A,E) (—) High, (- -) Low; Figures (B,F) (▭) CR/PR, (▭)PD/SD; Figure (C,G) Figure(D) (■) CR, (■)PD, (■)PR; Figure (H) (■) CR, (■) PD, (■) PR, (■) SD.

DISCUSSION

In this research, we included more than 1800 CRC patients in 6 cohorts for analysis. We used ssGSEA to calculate the NES of each patient, separately. The ssGSEA method does not rely on the influence of other samples in the gene expression datasets when scoring a single sample, and provides stable scores that are unlikely to be affected by different sample and gene sizes in the cohorts and unnecessary changes between samples. Thus, the ssGSEA score of each patient is less affected by the microarray platform of each cohort. The univariate Cox regression model results of 18 cohorts were analyzed by meta-analysis, and screening 48 immune related signatures. Finally, the IRPS of each patient is calculated through the NES of 48 signatures. Specifically, for each patient, we calculated the sum of the NES values of signatures with HRs less than 1 and HRs more than 1 respectively, and then the IRPS is equal to the subtraction of them.

In the 6 CRC datasets collected, most patients with the low IRPS showed better overall survival than those with the high IRPS. The results show that the IRPS can reflect the level of immune infiltration in the tumour microenvironment of CRC patients. The IRPS is negatively related to anti-tumour immune infiltrating cells and positively related to tumour immunosuppressive cells. It is well known that immunotherapy of CRC patients is closely related to microsatellite status and immune checkpoint molecules [11,14,27-29]. We confirmed the correlation between the IRPS and immunotherapy by analysing the relationship between the IRPS and microsatellite status. In addition, the potential mechanism of the IRPS affecting immunotherapy was explored based on genomic analysis. Among the many immunogenicity factors that affect the response to immunotherapy, TMB is a major factor, and TMB is related to the IRPS. At the same time, the relationship between the IRPS and other immunogenicity also further indicates that the IRPS may affect the response of immunotherapy by affecting immunogenicity [30].

In recent years, ICIs, such as anti-PD-1, anti-PD-L1 or anti-CTLA-4 therapy, in patients with solid tumours has aroused great interest in immunotherapy. Nevertheless, only a few patients have a long and stable response during immune checkpoint inhibiters treatment. Lately, TMB and the expression level of PD-1 and PD-L1 have been found not to be effective biomarkers to predict the benefits of immune checkpoint blocking [31]. Therefore, it is necessary to develop a useful tool to predict the efficacy of immunotherapy. In this study, the predictive ability of the IRPS for checkpoint

inhibitors was demonstrated in two groups of advanced melanoma and bladder cancer patients treated with anti-PD-1 antibody and anti-CTLA4 antibody, respectively. Our results distinctly show that the IRPS is associated with the response to different immunotherapy methods, including immunotherapy based on anti-PD-1, anti-PD-L1 and CTLA4 immune checkpoint inhibitors. The prediction accuracy of the two groups of patients indicated that the IRPS value can be used as a tool to evaluate the effectiveness of immunotherapy for cancer. The IRPS of patients who responded to immunotherapy were significantly lower than that of patients who did not respond to immunotherapy. Owing to the lack of a CRC cohort receiving immunotherapy, more prospective trials are needed to further validate these findings in patients with CRC.

There are still some deficiencies in this study. First, we obtained as many CRC cohorts as possible, but still did not find a suitable CRC immunotherapy cohort. We also need to conduct more experimental studies on immune related signatures, in order to provide more available information for further understanding their function in CRC. Finally, we only use the best cut-off of the IRPS to classify CRC samples into high IRPS subtype and low IRPS subtype, however, no other grouping method is used. We still need to find better cut-off values to provide a better strategy for stratification of CRC patients.

The IRPS is a valuable signature related to the level of immune infiltration. The correlation between the IRPS and the overall survival rate of CRC comprehensive cohort proves that the IRPS is a powerful prognostic hallmark of CRC. The IRPS should contribute to further determining the prognosis of patients with CRC and predict the response of patients with CRC to immunotherapy.

CONCLUSION

The IRPS is a valuable signature related to the level of immune infiltration. The correlation between the IRPS and the overall survival rate of CRC comprehensive cohort proves that the IRPS is a powerful prognostic hallmark of CRC. The IRPS should contribute to further determining the prognosis of patients with CRC and predict the response of patients with CRC to immunotherapy.

ACKNOWLEDGEMENT

The authors would like to thank TCGA, PubMed and GEO projects for the data access. Thanks to Research Square for allowing us to publish a preprint of the manuscript.

FUNDING

This work was supported by the National Nature Science Foundation of China (grant number 62276084), Central support for the reform and development of local colleges and universities (high-level talent project) (grant number 2020GSP05), Heilongjiang Province Applied Technology Research and Development Plan Project (GA19C003) and the National Natural Science Foundation of China Youth Science Fund Project (grant number 82103030).

COMPETING INTEREST

The authors have no relevant financial or non-financial interests to disclose.

DATA AVAILABILITY

The datasets analysed during the current study are available in the Gene Expression Omnibus (GEO) and The Cancer Genome Atlas (TCGA) repository. The web link of GEO is https://www.ncbi.nlm.nih.gov/geo/, datasets in GEO includes GSE12945, GSE17538, GSE39582, GSE103479 and GSE106584. The web link of TCGA is https://portal.gdc.cancer.gov/repository.

AUTHOR CONTRIBUTIONS

All authors contributed to the study conception and design. Material preparation, data collection and analysis were performed by Jun Xiang, JunHu Li and XiaoNan Cheng. The first draft of the manuscript was written by Jun Xiang and all authors commented on previous versions of the manuscript. All authors read and approved the final manuscript.

CONFLICT OF INTEREST STATEMENT

The authors confirm that there are no conflicts of interest.

ETHICS APPROVAL

This study was performed in line with the principles of the Declaration of Helsinki. Approval was granted by the Ethics Committee of Harbin Medical University.

REFERENCES

1. Sung H, Ferlay J, Siegel RL, Laversanne M, Soerjomataram I, Jemal A, et al. Global cancer statistics 2020: GLOBOCAN estimates of incidence and mortality worldwide for 36 cancers in 185 countries. CA Cancer J Clin. 2021;71(3):209-249.
2. Zheng R, Zhang S, Zeng H, Wang S, Sun K, Chen R, et al. Cancer incidence and mortality in China, 2016. Journal of the National Cancer Center. 2022;2(1):1-9.
3. He X, Xu C. Immune checkpoint signaling and cancer immunotherapy. Cell Res. 2020;30(8):660-669.
4. Belli C, Trapani D, Viale G, D'Amico P, Duso BA, Della Vigna P, et al. Targeting the microenvironment in solid tumors. Cancer Treat Rev. 2018;65:22-32.
5. Hinshaw DC, Shevde LA. The tumor microenvironment innately modulates cancer progression. Cancer Res. 2019;79(18):4557-4566.
6. Meng J, Zhou Y, Lu X, Bian Z, Chen Y, Zhou J, et al. Immune response drives outcomes in prostate cancer: Implications for immunotherapy. Mol Oncol. 2021;15(5):1358-1375.
7. Clemente CG, Mihm Jr MC, Bufalino R, Zurrida S, Collini P, Cascinelli N. Prognostic value of tumor infiltrating lymphocytes in the vertical growth phase of primary cutaneous melanoma. Cancer: Interdisciplinary International Journal of the American Cancer Society. 1996;77(7):1303-1310.
8. Van der Leun AM, Thommen DS, Schumacher TN. CD8$^+$ T cell states in human cancer: insights from single-cell analysis. Nat Rev Cancer. 2020;20(4):218-232.
9. Halle S, Keyser KA, Stahl FR, Busche A, Marquardt A, Zheng X, et al. In vivo killing capacity of cytotoxic T cells is limited and involves dynamic interactions and T cell cooperativity. Immunity. 2016;44(2):233-245.
10. Ganesh K, Stadler ZK, Cercek A, Mendelsohn RB, Shia J, Segal NH, et al. Immunotherapy in colorectal cancer: rationale, challenges and potential. Nat Rev Gastroenterol Hepatol. 2019;16(6):361-375.
11. Diaz LA, Le DT. PD-1 blockade in tumors with mismatch-repair deficiency. N Engl J Med. 2015;373(20):1979.
12. Chan TA, Wolchok JD, Snyder A. Genetic basis for clinical response to CTLA-4 blockade in melanoma. N Engl J Med. 2015;373(20):1984.
13. Rizvi NA, Hellmann MD, Snyder A, Kvistborg P, Makarov V, Havel JJ, et al. Mutational landscape determines sensitivity to PD-1 blockade in non–small cell lung cancer. Science. 2015;348(6230):124-128.

14. Asaoka Y, Ijichi H, Koike K. PD-1 Blockade in Tumors with Mismatch-Repair Deficiency. N Engl J Med 2015;373(20):1979.

15. Leek JT, Johnson WE, Parker HS, Jaffe AE, Storey JD. The sva package for removing batch effects and other unwanted variation in high-throughput experiments. Bioinformatics. 2012;28(6):882-883.

16. Mariathasan S, Turley SJ, Nickles D, Castiglioni A, Yuen K, Wang Y, et al. TGFβ attenuates tumour response to PD-L1 blockade by contributing to exclusion of T cells. Nature. 2018;554(7693):544-548.

17. Wolf DM, Lenburg ME, Yau C, Boudreau A, van't Veer LJ. Gene co-expression modules as clinically relevant hallmarks of breast cancer diversity. PloS one. 2014;9(2):e88309.

18. Kondratova M, Czerwinska U, Sompairac N, Amigorena SD, Soumelis V, Barillot E, et al. A multiscale signalling network map of innate immune response in cancer reveals cell heterogeneity signatures. Nat Commun. 2019;10(1):4808.

19. Godec J, Tan Y, Liberzon A, Tamayo P, Bhattacharya S, Butte AJ, et al. Compendium of immune signatures identifies conserved and species-specific biology in response to inflammation. Immunity. 2016;44(1):194-206.

20. Bindea G, Mlecnik B, Tosolini M, Kirilovsky A, Waldner M, Obenauf AC, et al. Spatiotemporal dynamics of intratumoral immune cells reveal the immune landscape in human cancer. Immunity. 2013;39(4):782-795.

21. Sanchez-Vega F, Mina M, Armenia J, Chatila WK, Luna A, La KC, et al. Oncogenic signaling pathways in the cancer genome atlas. Cell. 2018;173(2):321-337.

22. Cursons J, Souza-Fonseca-Guimaraes F, Foroutan M, Anderson A, Hollande F, Hediyeh-Zadeh S, et al. A Gene Signature Predicting Natural Killer Cell Infiltration and Improved Survival in Melanoma PatientsA Gene Signature for NK Infiltration and Melanoma Survival. Cancer Immunol Res. 2019;7(7):1162-1174.

23. Zhao B, Wang Y, Wang Y, Dai C, Wang Y, Ma W. Investigation of genetic determinants of glioma immune phenotype by integrative immunogenomic scale analysis. Front Immunol. 2021;12:557994.

24. Thompson JC, Davis C, Deshpande C, Hwang WT, Jeffries S, Huang A, et al. Gene signature of antigen processing and presentation machinery predicts response to checkpoint blockade in non-small cell lung cancer (NSCLC) and melanoma. J Immunother Cancer. 2020;8(2).

25. Danilova L, Ho WJ, Zhu Q, Vithayathil T, De Jesus-Acosta A, Azad NS,et al. Programmed cell death ligand-1 (PD-L1) and CD8 expression profiling identify an immunologic subtype of pancreatic ductal adenocarcinomas with favorable survival. Cancer Immunol Res. 2019;7(6):886-895.

26. Schreiber RD, Old LJ, Smyth MJ. Cancer immunoediting: integrating immunity's roles in cancer suppression and promotion. Science. 2011;331(6024):1565-1570.

27. Mlecnik B, Bindea G, Angell HK, Maby P, Angelova M, Tougeron D, et al. Integrative analyses of colorectal cancer show immunoscore is a stronger predictor of patient survival than microsatellite instability. Immunity. 2016;44(3):698-711.

28. Ferris RL, Lenz HJ, Trotta AM, García-Foncillas J, Schulten J, Audhuy F, et al. Rationale for combination of therapeutic antibodies targeting tumor cells and immune checkpoint receptors: Harnessing innate and adaptive immunity through IgG1 isotype immune effector stimulation. Cancer Treat Rev. 2018;63:48-60.

29. Jenkins RW, Barbie DA, Flaherty KT. Mechanisms of resistance to immune checkpoint inhibitors. Br J Cancer. 2018;118(1):9-16.

30. Goodman AM, Kato S, Bazhenova L, Patel SP, Frampton GM, Miller V, et al. Tumor mutational burden as an independent predictor of response to immunotherapy in diverse cancerstmb predicts response to immunotherapy in diverse cancers. Mol Cancer Ther. 2017;16(11):2598-2608.

31. Roh W, Chen PL, Reuben A, Spencer CN, Prieto PA, Miller JP, et al. Integrated molecular analysis of tumor biopsies on sequential CTLA-4 and PD-1 blockade reveals markers of response and resistance. Sci Transl Med. 2017;9(379):eaah3560.